Materials and Design 95 (2016) 632–640

Contents lists available at ScienceDirect

Materials and Design

journal homepage: www.elsevier.com/locate/matdes

Functionalization of polyacrylonitrile nanofibers with β-cyclodextrin for the capture of formaldehyde

Daniel Noreña-Caro, Mónica Álvarez-Láinez *

Product Design Engineering Department, Universidad EAFIT, Carrera 49 N 7sur-50, 050022 Medellin, Colombia

ARTICLE INFO

Article history:
Received 31 August 2015
Received in revised form 19 January 2016
Accepted 21 January 2016
Available online 1 February 2016

Keywords:
Polyacrylonitrile
β-Cyclodextrin
Nanofibers
Functionalization
Formaldehyde

ABSTRACT

Polyacrylonitrile (PAN) is frequently used in filtering applications due to its sound mechanical properties, chemical resistance and thermal stability. β-cyclodextrin (βCD) can entrap molecules and improve the filters' performance. The removal of formaldehyde, a common indoor pollutant, has increasingly attracted widespread attention. In this work, we present two different methods for the production of electrospun PAN nanofibers containing βCD capable of capturing formaldehyde from the air. The former comprised the addition of βCD to PAN/dimethyl sulfoxide solutions and the subsequent electrospinning of the mixture. The latter involved the crosslinking of βCD on electrospun PAN fibers by alkaline hydrolysis and esterification with citric acid. For both methods, we used solutions with different polymer concentration and viscosity. In addition, the rheology of solutions, as well as the morphology, surface area, chemical structure and thermal resistance of electrospun fibers were analyzed. The formaldehyde capture potential of βCD containing PAN nanofibers was evaluated using high performance liquid chromatography. Conclusively, we found that, while functionalized PAN nanofibers with average fiber diameter from 432 nm to 647 nm might be used for indoor air purification, functionalized fibers obtained by addition of βCD are more effective for capturing formaldehyde than fibers obtained by crosslinking of βCD.

1. Introduction

The reduction of indoor air pollution is important for minimizing the risks on human health. One of the most hazardous contaminants commonly found in the atmosphere is formaldehyde, a volatile organic compound (VOC) coming from paints, textiles, furniture binders, decorating materials and cigarette smoke [1,2]. Formaldehyde is considered harmful because it can produce ocular and nasal irritation, headache, nausea, rhinitis, pharyngitis, emphysema, asthma and lung cancer even when its concentration in the air reaches 20 ppm or less [1–3]. To maintain a safe atmosphere at the inside of buildings, the concentration of indoor formaldehyde should be kept under its permissible exposure limit (PEL) of 0.75 ppm within a period of 8 h [4].

Currently, modified activated carbon fibers (ACF) derived from polyacrylonitrile (PAN) are considered among the most promising adsorbents for capturing formaldehyde. The remarkable adsorption capacity of PAN derived ACF is due to their microporous structure and chemical composition. While the microporous structure provides a large active surface area, the nitrogen containing groups on the surface of PAN derived ACF enhance the chemical affinity between the adsorbent and the formaldehyde [2,3,5]. In addition, this affinity is improved when ACF are functionalized with hydrophilic functional groups such as hydroxyl (OH), carbonyl ($\mathrm{C{=}O}$) and ether ($\mathrm{C{-}O}$) [6].

Although polymer nanofiber fabrics manufactured by electrospinning have less surface area than ACF, we believe that they could also be considered as potential adsorbents of formaldehyde after functionalization with suitable molecules such as β-cyclodextrin (βCD) [7]. These fibers can be used in air filtration applications because they have large surface to volume ratio, high surface cohesion, high porosity and suitable mechanical performance [8–10]. Given that PAN is the raw material for the production of ACF, and that βCD is a source of hydrophilic hydroxyl groups, the functionalization of electrospun PAN nanofibers with βCD could result in an effective and cheaper material for capturing airborne formaldehyde.

βCD is a toroid shaped cyclic oligosaccharide consisting of seven units of 1,4-linked glucopyranosides [11]. Due to its external hydrophilic groups (hydroxyl) and its hydrophobic inner cavity, it can form host-guest complexes with organic molecules and has gained attention as potential polymer additive for environmental applications [12–20]. One of these applications describes the promising properties of cyclodextrin functionalized electrospun poly methyl methacrylate (PMMA) nanofibers as molecular filter for styrene, aniline and toluene vapors [12]. A different study reports, that βCD included in the nanofiber fabric improved the entrapment capacity of aniline in vapor phase by polyethylene terephthalate (PET) [15].

---

* Corresponding author.
E-mail address: malvar26@eafit.edu.co (M. Álvarez-Láinez).

http://dx.doi.org/10.1016/j.matdes.2016.01.106

In this work, we compare two methodologies for the manufacturing of electrospun PAN nanofibers functionalized with βCD. The first approach consists of the addition of βCD to the polymer solution before electrospinning. With this physical functionalization method, only low energy bonds between the PAN nanofibers and the cyclodextrin are created. The second method comprises a crosslinking process involving two steps. In the first step, the PAN nanofibers are modified by alkaline hydrolysis to generate a backbone with reactive carboxylic groups [21–24]. Subsequently, a solution containing citric acid (CA) and βCD is added to promote an esterification reaction with the modified PAN fibers [14,19,25–27]. This chemical functionalization process generates stronger covalent bonds between the polymer and the βCD. This turns into a better attachment of the cyclodextrin to the nanofiber. To define the best route for the functionalization of PAN nanofibers with βCD, our experimental approach takes into consideration the differences in fiber morphology, chemical composition, thermal resistance, surface area, porous structure and formaldehyde capture potential of physically and chemically functionalized nanofibers.

2. Experimental

2.1. Materials

PAN powder with a molecular weight of 150.000 g/mol was obtained from Scientific Polymer Products Inc. and βCD powder (Cavamax W7) was kindly provided by Wacker Chemie AG. Dimethyl sulfoxide (DMSO, 99.9%, Carlo Erba Reagents) was used for preparing polymer solutions. Solid potassium hydroxide (KOH, 90%, Ashta Chemicals Inc.), sodium hypophosphite (SHP, 99.5%, Special Materials Company), citric acid (CA, 99.5%, Sigma Aldrich) and deionized water were used for the chemical functionalization process. For the formaldehyde capture evaluation, formalin solution (37.6% Formaldehyde, Panreac), acetonitrile (99.8% pure, Sigma Aldrich), 2,4-dinitrophenyl hydrazine (2,4-DNPH 70%, Sigma Aldrich), glacial acetic acid (99%, Sigma Aldrich) and sodium acetate (99%, Sigma Aldrich) were used. All the materials were used as received without further purification.

2.2. Solutions preparation

For preparing polymer nanofibers with different average diameters, polymer solutions in DMSO with concentrations of 5% *w*/w, 7% *w*/w and 9% *w*/w were prepared. The physical functionalization of PAN nanofibers was made by adding 10% *w*/w βCD to the polymer solution during the solution preparation. The βCD percentage was based on the polymer content (solvent free). The solutions were stirred at 500 rpm for 12 h at room temperature and immediately electrospun. A total of six different solutions were prepared (PAN 5%/DMSO, PAN 5%/DMSO/βCD, PAN 7%/DMSO, PAN 7%/DMSO/βCD, PAN 9%/DMSO and PAN 9%/DMSO/βCD).

2.3. Polymer solution viscosity

The rheology of PAN/DMSO and PAN/DMSO + βCD polymer solutions was analyzed using a rotational rheometer model Haake Mars III (Thermo Fisher Scientific). A concentric geometry Z20DIN was used and the flow sweeps were conducted at 25 °C varying the shear rate between 0.1 s^{-1} and 1500 s^{-1}.

2.4. Production of electrospun PAN nanofibers

A horizontal electrospinning array was used for the production of electrospun PAN fabrics with different average diameters. Electrospinning of different polymer solutions was executed in a room at 22 °C and 55% relative humidity using the following process conditions: applied voltage (10 kV), flow rate (0.5 ml/h) and tip to collector distance (12 cm). The electrospun volume of each solution was varied depending on the PAN concentration in order to obtain nanofiber fabrics with homogeneous weight (1.78 ml for PAN 5%/DMSO, 1.27 ml for PAN 7%/DMSO and 1.00 ml for PAN 9%/DMSO). The electrospun nanofibers were vacuum dried for 12 h at 45 °C and 200 mBar absolute pressure before being detached from the aluminium foil.

2.5. Functionalization process

Physically functionalized PAN nanofibers (PAN/βCD) with different average diameters were produced using the same electrospinning conditions defined for PAN nanofibers. However, the electrospun nanofibers were produced from the polymer solutions with added βCD (PAN 5%/DMSO/βCD, PAN 7%/DMSO/βCD and PAN 9%/DMSO/βCD).

Chemically functionalized PAN nanofibers (PAN/CA-βCD) with different average diameters were obtained by modifying electrospun PAN nanofibers. The changes on the chemical structure of PAN nanofibers were observed using attenuated total reflectance Fourier transformed infrared Spectroscopy (Spectrum Two ATR-FTIR Spectrometer, Perkin Elmer). The change on the chemical structure of the nanofibers was identified by observing the peak area of the different functional groups involved in the functionalization process. Peak areas were calculated by adjusting the absorbance vs wave number information to Gaussian curves.

The first step for chemical functionalization consisted of the partial hydrolysis of PAN nanowebs in a sealed polyethylene bag with 5% *w*/w KOH aqueous solution (1:3750 polymer to solution weight ratio). The bags were immersed in a thermostatic bath at 60 °C. The reaction proceeded for 2 h and, after that time, partially hydrolyzed and yellowish PAN fibers were removed and washed with tap water for one minute. Because of the alkaline hydrolysis, some nitrile groups (CN) on the polymer turn into amide ($CONH_2$) and carboxylic acid (COOH) groups [21]. The second step involved the esterification of the hydroxyl (OH) groups in βCD and CA with the carboxylic groups in CA and the partially modified PAN. For making this, an aqueous solution with 2% *w*/w βCD, 0.7% *w*/w CA and 0.2% *w*/w SHP (catalyst) was prepared at 50 °C and mixed for homogenization for 30 min [19]. The washed and hydrolyzed PAN nanofiber fabrics were put with the solution of βCD, CA and SHP in another sealed polyethylene bag (1:1050 polymer to solution weight ratio) and immersed in a thermostatic bath at 60 °C. The esterification — cross-linking reaction proceeded for 2 h. After the reaction, esterified PAN fibers were removed, dried at 105 °C for 10 min and cured at 170 °C for 3 min. The yellowish color of the modified PAN fibers disappeared after the esterification step. Fig. 1 presents different alternatives for the formation of covalent bonds between the hydroxyl (OH) and carboxylic acid (COOH) groups that are present in the modified PAN, βCD and citric acid molecules.

2.6. Characterization of nanofibers

The morphology and diameter distribution of PAN, PAN/βCD and PAN/CA-βCD nanofibers were observed after gold metallization using a field emission scanning electron microscope (FESEM model Schottky JSM-7100F, JEOL Ltd.). The FESEM pictures of the nanofibers were analyzed using the ImageJ software and the diameter of 50 fibers per sample was measured for obtaining the diameter distribution.

A thermogravimetric analyzer TGA Q500 (TA Instruments) was used to investigate the changes on the thermal resistance of PAN nanofibers due to the functionalization. Samples were heated from 25 C to 900 C at a heating rate of 20 C/min under Nitrogen atmosphere.

The surface area and pore volume of unmodified and functionalized PAN nanofibers were measured by programming Nitrogen Adsorption Isotherms in a NOVA 2200e sorptometer (Quantachrome Instruments). Prior to Nitrogen adsorption analysis, the different nanofiber samples were subjected to vacuum degasification for 1.5 h at 160 C. The analysis was conducted using 9 mm outer diameter cells with bulb ending. The surface area of each sample was calculated using the BET (Brunauer–Emmett–Teller) method that takes into consideration the amount of

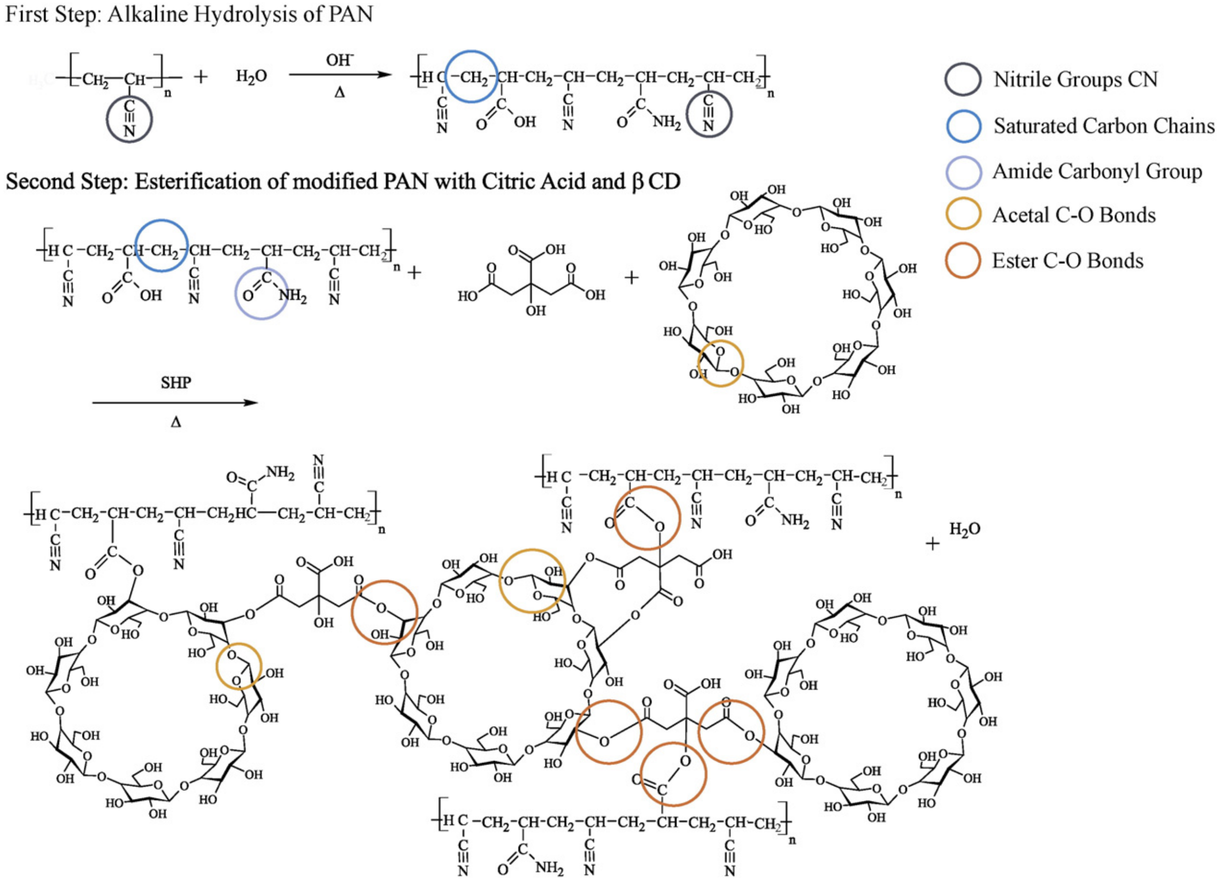

Fig. 1. Proposed chemical reactions in the chemical functionalization of PAN nanofibers with βCD.

nitrogen adsorbed at low pressure levels from 0.05 to 0.33 P/Po (Po is the absolute atmosphere pressure). The volume of mesopores and micropores in the nanofibers was characterized using the BJH (Barret–Joyner–Halenda) and HK (Horváth–Kawazoe) methods that consider the amount of nitrogen adsorbed at high pressure levels from 0.33 to 0.99 P/Po.

2.7. Formaldehyde capture evaluation

Nanofibrous fabrics were tested in an atmosphere with a formaldehyde concentration above the permissible exposure limit [4]. An atmosphere with 3 ppm formaldehyde was created by placing a glass Petri dish with 0.15 ml of formalin solution in a glass desiccator (33 cm diameter, 26.5 cm height and approximate volume of 16.6 l). The desiccator was kept sealed until complete evaporation of the formaldehyde solution drops. After creating the formaldehyde atmosphere, 10 ± 0.5 mg samples of PAN, PAN/βCD and PAN/CA-βCD with different average fiber diameter were positioned in the desiccator at 13 cm over the bottom of the container. The nanofibers were left in the desiccator for 4, 8 and 12 h. Once the contact times were over, the nanofiber samples were removed and their formaldehyde content was extracted with deionized water at 40 °C for one hour. According to the US-EPA (U.S Environmental Protection Agency) method 8315 [28], the extracted formaldehyde was derivatized with excess 2,4-DNPH in a 5.0 pH medium created with sodium acetate and acetic acid. The derivatization process occurred at 40 °C for one hour for total conversion of the aldehyde to the corresponding formaldehyde hydrazone.

After derivatization, the solutions were filtered using syringe filters with pore size of 0.45 m and the formaldehyde hydrazone concentration was measured using high performance liquid chromatography (HPLC — Agilent Technologies 1200 series). The sample components were separated using a Zorbax Eclipse XDB-C18 (4.6 mm × 250 mm, 5 μm) column and analyzed using UV–visible detection at 349 nm. The mobile phase was 70% *v*/v acetonitrile — 30% *v*/v water, the flow rate was 0.8 ml/min and the injection volume was 20 μl. The excess 2,4-DNPH peak was observed after 4 min from the beginning, the formaldehyde hydrazone peak was observed after 5 min of elution and the total run time was 6 min. The amount of formaldehyde adsorbed by PAN, PAN/βCD and PAN/CA-βCD nanofibers after the different contact times was determined from the area of the derivatized formaldehyde hydrazone peak observed in the HPLC chromatograms. For the quantification, the calibration curve (peak area vs concentration) was generated using formaldehyde hydrazone solutions (0.1 ppm, 0.15 ppm, 0.2 ppm, 0.4 ppm, 0.8 ppm, 2.0 ppm, 5.0 ppm and 10.0 ppm) and an R^2 correlation coefficient of 0.9992 was obtained. The measurements of the analyte of interest were repeated three times for each sample.

3. Results and discussion

3.1. Solution viscosity

We carried out flow sweeps of the polymer solutions to establish a relationship between the viscosity of the electrospinning fluid and the fiber diameter that could be obtained from these solutions. We wanted to observe if changes in the diameter or morphology of unmodified and functionalized nanofibers would affect their porous structure and their formaldehyde capture potential. Flow sweeps of the six different solutions used for electrospinning are presented in Fig. 2.

For all the solutions, the flat viscosity region can be seen between 0.1 s^{-1} and 10 s^{-1} shear rates. Considering the inner diameter (0.603 mm) of the needle and the flow rate of the polymer solution in the capillary (0.5 ml/h), the apparent shear rate applied by the syringe

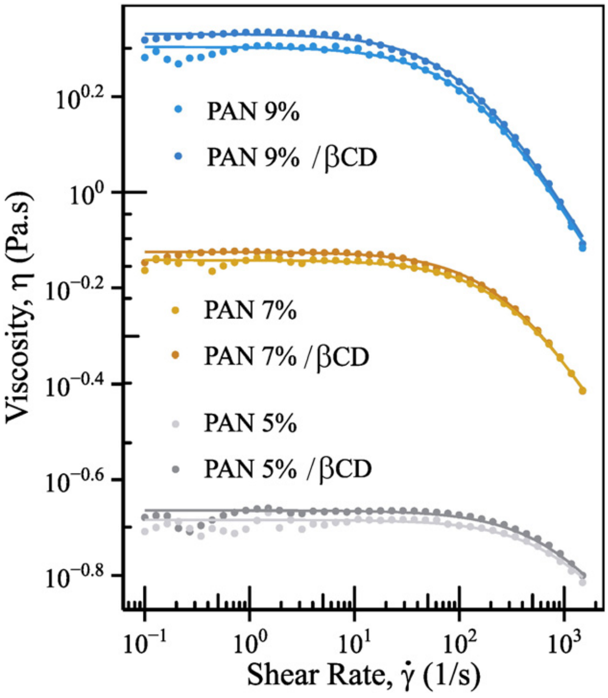

Fig. 2. Flow sweeps for PAN/DMSO and PAN/DMSO + β-CD polymer solutions.

plug during the spinning process is 6.44 s^{-1}. Based on this, we conducted the electrospinning of PAN and PAN/βCD nanofibers under low shear rate conditions with non-significant change (Newtonian plateau) on the viscosity of the polymer solutions.

Because of the higher content of solids and large chain molecules, the viscosity of the polymer solutions at the apparent shear rate (6.44 s^{-1}) increased with the polymer concentration. Based on the shape of the flow sweep curves, it can be said that PAN/DMSO and PAN/DMSO/βCD polymer solutions have a more pronounced pseudoplastic rheological behavior when the PAN concentration is increased. Besides, when the PAN concentration is increased, there is a reduction on the shear rate that is needed for the transition from the Newtonian plateau to the pseudoplastic region. These observations are consistent with our previous work [20] and they should be taken into consideration if it is desired to produce electrospun nanofibers using more concentrated polymer solutions at higher flow rates. Although the addition of βCD augmented the viscosity of each solution at the different PAN concentrations, the rheological behavior of the polymer solutions was not modified. The estimated viscosity of PAN 5%/DMSO/βCD was 4.64% higher than PAN 5%/DMSO solution viscosity, the viscosity of PAN 7%/DMSO/βCD was 3.91% higher than PAN 7%/DMSO solution viscosity and there was a raise of 6.24% in the viscosity when βCD was added to PAN 9%/DMSO polymer solution.

3.2. Functionalization of PAN nanofibers

Fig. 3 presents the results of the infrared spectroscopy for PAN, PAN/βCD and PAN/CA-βCD nanofibers. The FTIR spectrum for β-CD powder is also included. We identified changes on the nanofiber chemical composition during the functionalization by observing the intensity of the peaks at 2243 cm^{-1} and 1450 cm^{-1}. These peaks correspond to the stretching of the nitrile (CN) group and the bending of the saturated Carbons (CH_2) in the PAN molecule. The peak at 1033 cm^{-1} represents the stretching of the C—O bonds of the acetal group in the glucopyranoside units of the βCD molecule. Besides, additional C—O bonds are formed during the esterification step of the βCD crosslinking process.

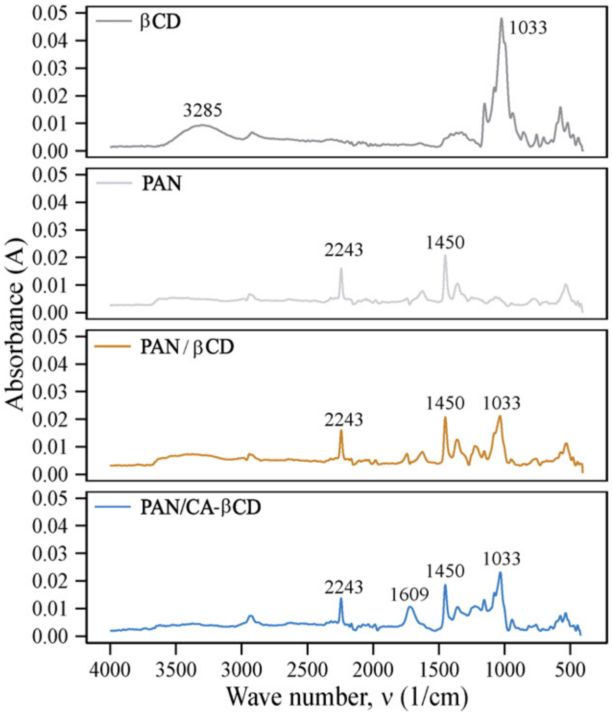

Fig. 3. FTIR spectra of PAN, βCD and functionalized nanofibers.

In the first step of the chemical functionalization, some nitrile groups should turn into amide ($CONH_2$) and carboxylic acid groups (COOH) (see Fig. 1). To confirm the chemical modification of the nitrile groups in the PAN/CA-βCD nanofibers, the nitrile index for these samples was compared with the nitrile index of the samples that were not subjected to chemical functionalization (PAN and PAN/β-CD). This index was calculated as the ratio between the peak area associated to nitriles in the spectra and the peak area of an invariant peak. The peak selected as constant was the one related to the bending of saturated carbon chains (CH_2) at 1450 cm^{-1} because this part of the molecule is not affected during the hydrolysis reaction and its intensity does not change during the chemical modification. The nitrile indexes for the FTIR spectra of PAN, PAN/βCD and PAN/CA-βCD nanofibers are presented in Table 1 and it can be observed that the nitrile index of the chemically functionalized sample (PAN/CA-βCD) is 16.5% lower than the nitrile index for the unmodified polymer nanofiber (PAN). This difference is evidence of the reduction on the nitrile group content when the PAN nanofiber is chemically modified and the formation of new groups from the reacting nitriles can be seen at 1609 cm^{-1} (stretching of amide carbonyl) on the IR spectrum for the chemically functionalized nanofiber (PAN/CA-βCD). The reduction on the content of Nitrile groups is coherent with the results reported for the alkaline hydrolysis of PAN [21]. By comparing the nitrile index values for PAN and PAN/CD (physically functionalized), it can be seen that these values are very similar because there is no chemical reaction between the polymer and the cyclodextrin when the βCD is added to the polymer solution before the electrospinning process.

Table 1
Nitrile and Carbon–Oxygen indexes of PAN, PAN/βCD and PAN/CA-βCD nanofibers.

Fiber type	CH_2 PA[a] (A/cm)	CN PA (A/cm)	CN index	CO PA (A/cm)	CO index
PAN	0.3915	0.2089	0.5336	0.0715	0.1826
PAN/βCD	0.3883	0.2031	0.5230	0.8377	2.1571
PAN/CA-βCD	0.3855	0.1744	0.4523	0.8466	2.1960

[a] PA: Peak area.

In the second step of the chemical functionalization, the hydroxyl (OH) groups in the βCD and citric acid molecules reacted with carboxyl groups in the modified PAN and the citric acid to form an esterified cross-linked structure. The βCD content after the chemical and physical functionalization can be identified by observing the peaks at 1033 cm^{-1} (See Fig. 3). This peak is related to the stretching of the C—O groups in the cyclodextrin molecules. The intensity of the C—O peaks for the chemically (PAN/CA-βCD) and physically (PAN/βCD) functionalized nanofibers can be compared by the C—O Index from the corresponding FTIR spectra. This index corresponds to the ratio between the peak areas of the signal at 1033 cm^{-1} and the peak area of the constant signal associated to the bending of saturated carbon chains (CH$_2$) at 1450 cm^{-1}. Note that the spectrum contains multiple peaks around 1033 cm^{-1} and it was necessary to use a deconvolution function to estimate the peak area. The C—O indexes are presented in Table 1. βCD molecules are present in the functionalized PAN fibers because the C—O index of the chemically and physically functionalized nanofibers is higher than the same index for the unmodified PAN fibers. Index for PAN/βCD (physically functionalized) is slightly lower than the same index for PAN/CA-βCD (chemically functionalized) nanofibers. This difference makes sense because the C—O peak in the crosslinked nanofiber contains the C—O bonds in the acetal group of the βCD and in the crosslinked structure formed during the esterification with CA.

3.3. Morphology of nanofibers

Fig. 4 presents comparative boxplots of unmodified and βCD functionalized PAN nanofibers produced from polymer solutions in DMSO with 5%(*w*/w), 7%(*w*/w) and 9%(*w*/w) PAN concentration.

Using the information in Figs. 2 and 4, it is possible to establish the relationship between the polymer solution concentration and the diameter of the electrospun PAN nanofiber in a PAN concentration range from 5%(*w*/w) to 9%(*w*/w). As it is well known from the theory of the electrospinning process [29,30], the higher the concentration of the polymer solution, the higher the diameter of electrospun nanofibers. This effect can be explained considering that the polymer solutions with increased viscosity are more resistant to deformation when an external force, such as the electric force, is applied to elongate the droplet during the electrospun fiber formation. When the βCD is added to the polymer solution, the fiber diameter increasing effect is also observed when solutions with higher content of polymer are used. Moreover, the addition of cyclodextrin to the solution increases the content of solids, the viscosity of the solution, and the PAN/βCD nanofibers are thicker than the solely PAN nanofibers at the same PAN concentration. In the case of the chemically functionalized (PAN/CA-βCD) nanofibers, these fibers may be thicker than only PAN nanofibers because of the esterification among the PAN polymer, the CA and the βCD molecules. These bonds occur mainly on the surface of the fibers forming a cyclodextrin polymer coating that increases the apparent diameter of the fiber [19]. Considering the values of the average fiber diameters presented in Fig. 4, it can be stated that the functionalization increased the diameter of the electrospun PAN nanofibers. However, no significant difference was observed in the mean fiber diameter of the functionalized PAN nanofibers obtained by addition of βCD (PAN/βCD) and crosslinking of βCD (PAN/CA-βCD).

The average diameters of the PAN and PAN/βCD nanofibers at the selected polymer concentrations are coherent with the results from our previous work [20] and with the diameters of electrospun PAN nanofibers obtained from solutions in DMSO [31,32]. The average fiber diameters of these fibers obtained from polymer solutions in DMSO are higher than the diameter of electrospun PAN fibers manufactured from polymer solutions in Dimethylformamide (DMF) [33,34] because the PAN/DMSO solutions are more viscous and less volatile than PAN/DMF solutions at the same polymer concentration [35]. Representative SEM Images of PAN, PAN/βCD and PAN/CA-βCD nanofibers are presented in Fig. 5. As shown by all the pictures, bead free nanofibers were obtained at the selected electrospinning process conditions for all the polymer concentrations under observation. However, the shape and the surface of the nanofibers are more uniform for the fibers produced from 7% (*w*/w) and 9% (*w*/w) PAN electrospinning solutions, because the electrospinning process is more stable when the viscosity of the solution is high enough for maintaining the balance between the viscous and the electrical forces during the electrospun fiber formation, but low enough for avoiding the clogging of the syringe needle.

3.4. Surface area and pore volume of nanofibers

From Fig. 6, it can be seen that the lowest values of surface area correspond to the thickest fibers produced from polymer solution with 9% (*w*/w) PAN. On the other hand, the surface area of nanofibers is maximized when they are produced from polymer solutions with low PAN concentration (i.e. 5% (*w*/w) PAN). This was expected because the surface area to volume ratio of nanofibers is increased when the fiber diameter is reduced [36]. Additionally, it can be seen that the functionalization of PAN nanofibers with βCD reduces the surface

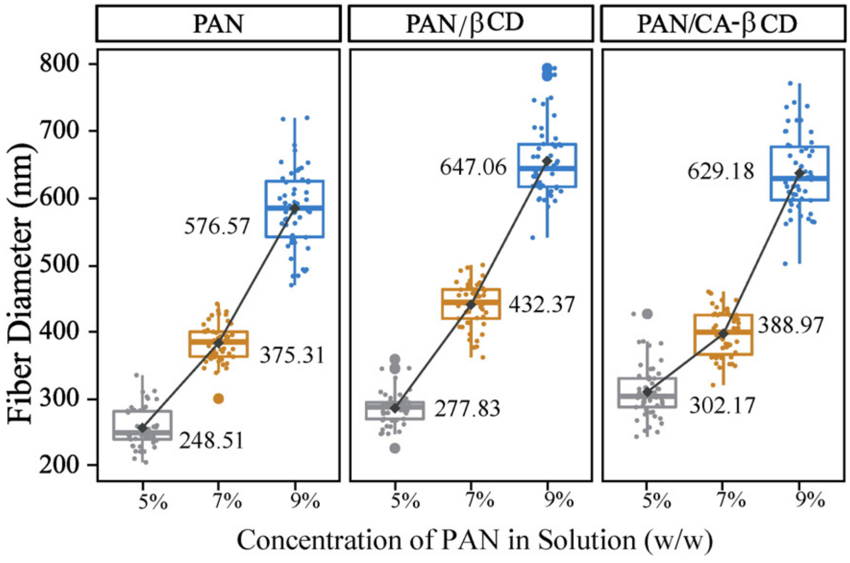

Fig. 4. Diameter distribution of PAN, PAN/βCD and PAN/CA-βCD nanofibers.

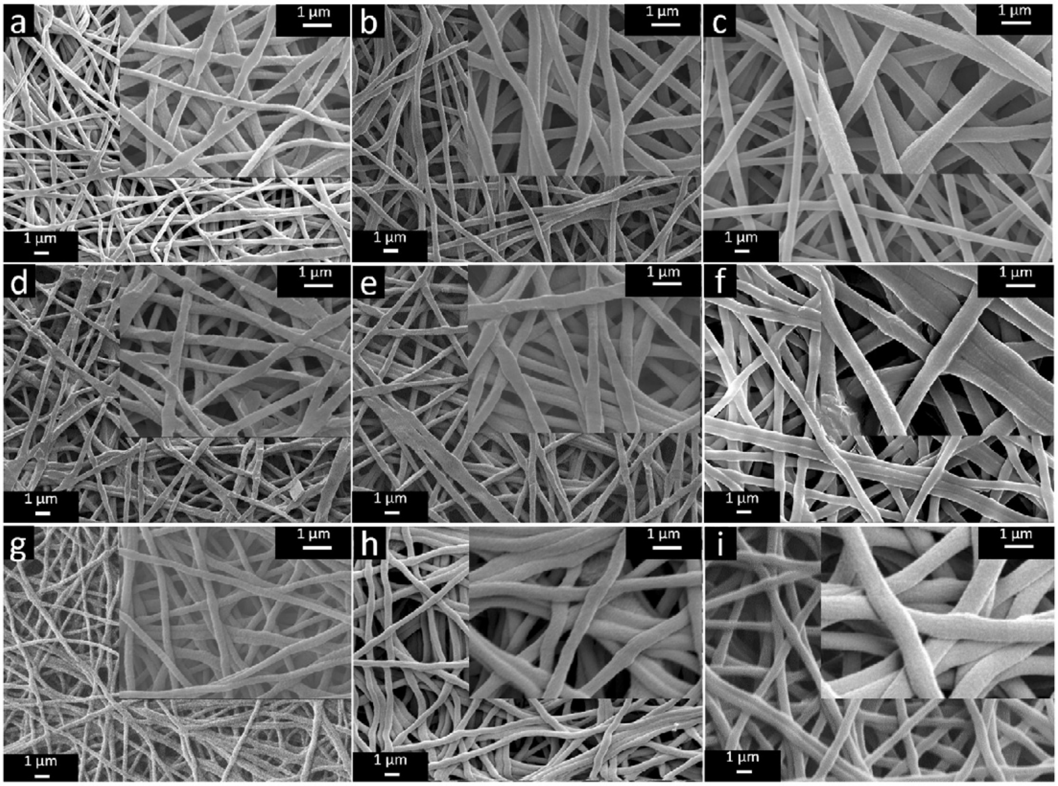

Fig. 5. SEM Images of nanofibers: (a)PAN 5%, (b)PAN 7%, (c)PAN 9%, (d)PAN 5%/βCD, (e)PAN 7%/βCD, (f)PAN 9%/βCD, (g)PAN 5%/CA-βCD, (h)PAN 7%/CA-βCD and (i)PAN 9%/CA-βCD.

area, and this reduction is higher for the chemically functionalized nanofibers.

Table 2 summarizes the results for the pore volume of mesopores and micropores estimated using the BJH and HK methods respectively. Based on these results, we found that unmodified and functionalized PAN nanofibers are mesoporous structures. Taking into consideration the pore volume of mesopores and micropores, the thickest nanofibers (i.e. produced from solutions containing 9% (*w*/w) PAN) are less porous than thinner nanofibers and this is coherent with the surface areas that were found for these fibers. In addition, both functionalization methods of electrospun PAN nanofibers reduced the pore volume of the nanofibers but the chemical functionalization (PAN/CA-βCD nanofibers) generated the highest reduction in the pore volume of micropores. Similar results have been also reported elsewhere [19] and this observation is important because the volume of the micropores may be related with the amount of small molecules (such as formaldehyde) that can be entrapped by the porous structure of the adsorbent.

3.5. Thermal stability

Fig. 7 presents the temperatures of the main degradation events for unmodified and functionalized nanofibers. Because the thermal resistance properties are not affected by the PAN nanofiber diameter, the TGA analysis was conducted on representative samples of PAN, PAN/βCD and PAN/CA-βCD nanofibers with different diameters.

The two main degradation events of βCD sample presented in Fig. 7 correspond to the complete loss of water contained in the hygroscopic cyclodextrin molecule at 99.23 °C and the complete thermal degradation

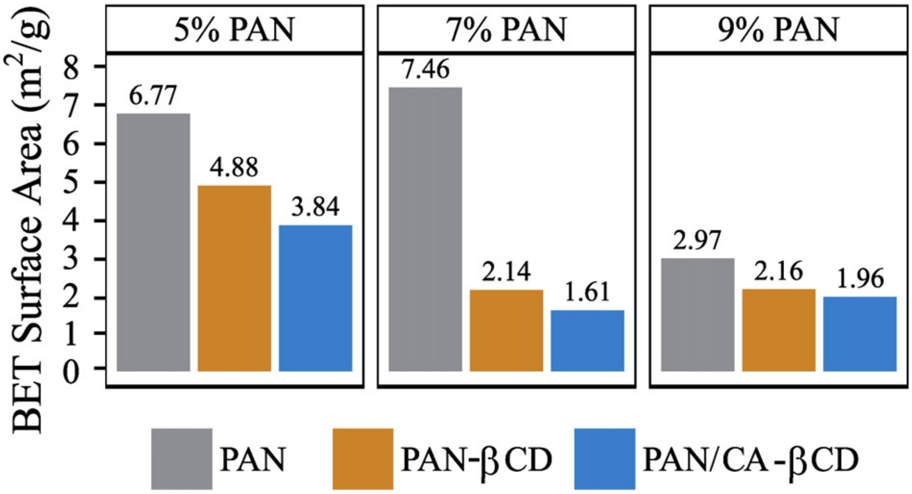

Fig. 6. Surface area of PAN, PAN/βCD and PAN/CA-βCD nanofibers.

Table 2
Surface area and pore volume of PAN, PAN/βCD and PAN/CA-βCD nanofibers.

Fiber type	PAN concent. (*w*/w)[a]	Mesopores BJH pore volume (cm^3/g)	Micropores HK pore volume (cm^3/g)
PAN	5%	0.0189	0.0019
PAN/βCD	5%	0.0202	0.0017
PAN/CA-βCD	5%	0.0178	0.0008
PAN	7%	0.0253	0.0030
PAN/βCD	7%	0.0133	0.0002
PAN/CA-βCD	7%	0.0106	0.0000[a]
PAN	9%	0.0160	0.0022
PAN/βCD	9%	0.0117	0.0015
PAN/CA-βCD	9%	0.0103	0.0005

[a] The volume of micropores is negligible and their average size is close to mesopores.

of the molecule at 320.85 °C. For the PAN sample, there is a first degradation event at 294.75 °C that is related to the loss of hydrogen (dehydrogenation reaction) in the PAN molecule and a second mass loss event at 692.70 °C associated to the loss of nitrogen as described for the process of carbon fiber production from polyacrylonitrile [36]. The physically functionalized PAN/βCD nanofibers presented two main mass loss events at 292.86 °C and 618.25 °C that are associated to the degradation of βCD and to the loss of hydrogen and nitrogen in the PAN molecule.

For the PAN/CA-βCD sample (chemically functionalized), there were found three degradation events at 226.66 °C (Citric acid degradation), 311.04 °C (β-CD degradation and dehydrogenation of PAN) and 583.98 °C (nitrogen loss in the PAN molecule). Based on these results, the functionalization of PAN nanofibers with βCD produces a reduction in the second degradation event (loss of nitrogen) of the polymer molecule. The reduction is more pronounced for the chemically functionalized fibers because the covalent bond between the polymer and cyclodextrin was conducted by modifying the chemical structure of nitrile groups to form amide and carboxyl groups. Considering the first degradation event of PAN, PAN/βCD and PAN/CA-βCD samples, the physical functionalization of PAN with βCD does not significantly affect the thermal resistance of the pristine PAN nanofibers. However, the chemical functionalization of PAN nanofibers with citric acid reduces the overall thermal resistance of the nanofiber fabric because the thermal degradation of the citric acid (main esterifying agent) occurs at lower temperatures than the degradation of the βCD and the PAN molecules [11,19,37].

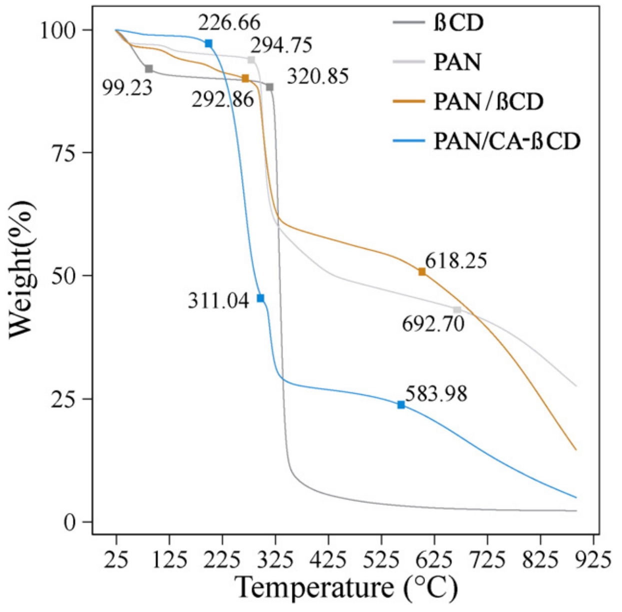

Fig. 7. TGA Analysis of βCD and PAN, PAN/βCD and PAN/CA-βCD nanofibers.

3.6. Formaldehyde capture evaluation

The chart in Fig. 8 presents the amount of formaldehyde captured per active surface of unmodified and functionalized PAN nanofibers. After 4 h of exposure, no difference on the formaldehyde capture potential of unmodified and functionalized fibers is observed for the thinnest fibers (obtained from 5% *w*/w PAN solutions). However, the effect of the functionalization process can be seen as thicker fibers are tested (obtained from 7% *w*/w and 9% *w*/w PAN solutions). It is clear that the functionalization process involving the addition of /βCD (PAN/βCD) results in a better activation of the PAN fiber surface as compared to the crosslinking functionalization method (PAN/CA-βCD).

Considering the amount of formaldehyde that has been captured after 8 h of exposure, the effect of the physical functionalization of PAN nanofibers with added βCD is remarkable. It can be seen, however, that the weight of formaldehyde per active surface of fiber that can be entrapped by chemically functionalized nanofibers (PAN/CA-βCD) is comparable to or even lower than the capturing potential of unmodified PAN fibers. Once again, the formaldehyde capture potential of physically functionalized fibers is even better for fibers that have been obtained from 7% *w*/w and 9% *w*/w PAN solutions (average fiber diameter between 432 nm and 647 nm).

Taking into consideration the results after 12 h of exposition, the physically functionalized nanofibers (PAN/βCD) have the best performance among all evaluated fibers. Once again, the capturing potential of the thickest fibers (7% *w*/w and 9% *w*/w PAN solutions) is superior and doubles the capturing potential of the thinnest fibers (5% *w*/w PAN). It is worth mentioning that the results for the chemically modified fibers (PAN/CA-βCD) improve after 12 h of exposure and their formaldehyde capturing potential is higher as compared to the unmodified fibers. However, it is still very clear that the functionalization method involving the addition of βCD is superior to the crosslinking functionalization method. Besides, the physically functionalized nanofibers are faster on capturing formaldehyde from the air. We believe that the addition functionalization method is better because of the hydroxyl (OH) groups that are present on the βCD molecule and that improve the formaldehyde capture potential [6].

Although the βCD was crosslinked to the polymer in the chemically functionalized PAN nanofibers (PAN/CA-βCD), the amount of formaldehyde entrapped by these fibers is, in some cases, lower than the quantity of contaminant captured by unmodified PAN fibers. This may have happened because the available surface and micropore volume for capturing the formaldehyde were minimal. In addition, the chemical functionalization requires the modification of nitrile groups in the polymer molecule and the esterification of the hydroxyl (OH) groups of the βCD molecules with citric acid (see Fig. 1). Because of the change on the chemical structure of OH groups, the affinity between functionalized PAN nanofibers and formaldehyde molecules is reduced. Based on these observations, and considering the high affinity between formaldehyde and hydrophilic groups [38], it can be stated that the capturing of this contaminant by the cyclodextrin molecule is conducted on the external hydrophilic part of the βCD. This observation differs from what has been reported in other works involving cyclodextrins [10–16], given that the inner hydrophobic part of the molecule may not be responsible of capturing the organic contaminant under evaluation.

4. Conclusions

The electrospinning of PAN nanofibers is a low shear rate process and fibers with sub-micron average fiber diameters may be obtained from polymer solutions in DMSO with PAN concentration from 5%(*w*/w) to 9%(*w*/w). These fibers may be physically or chemically functionalized with βCD and the functionalization increases the fiber diameter.

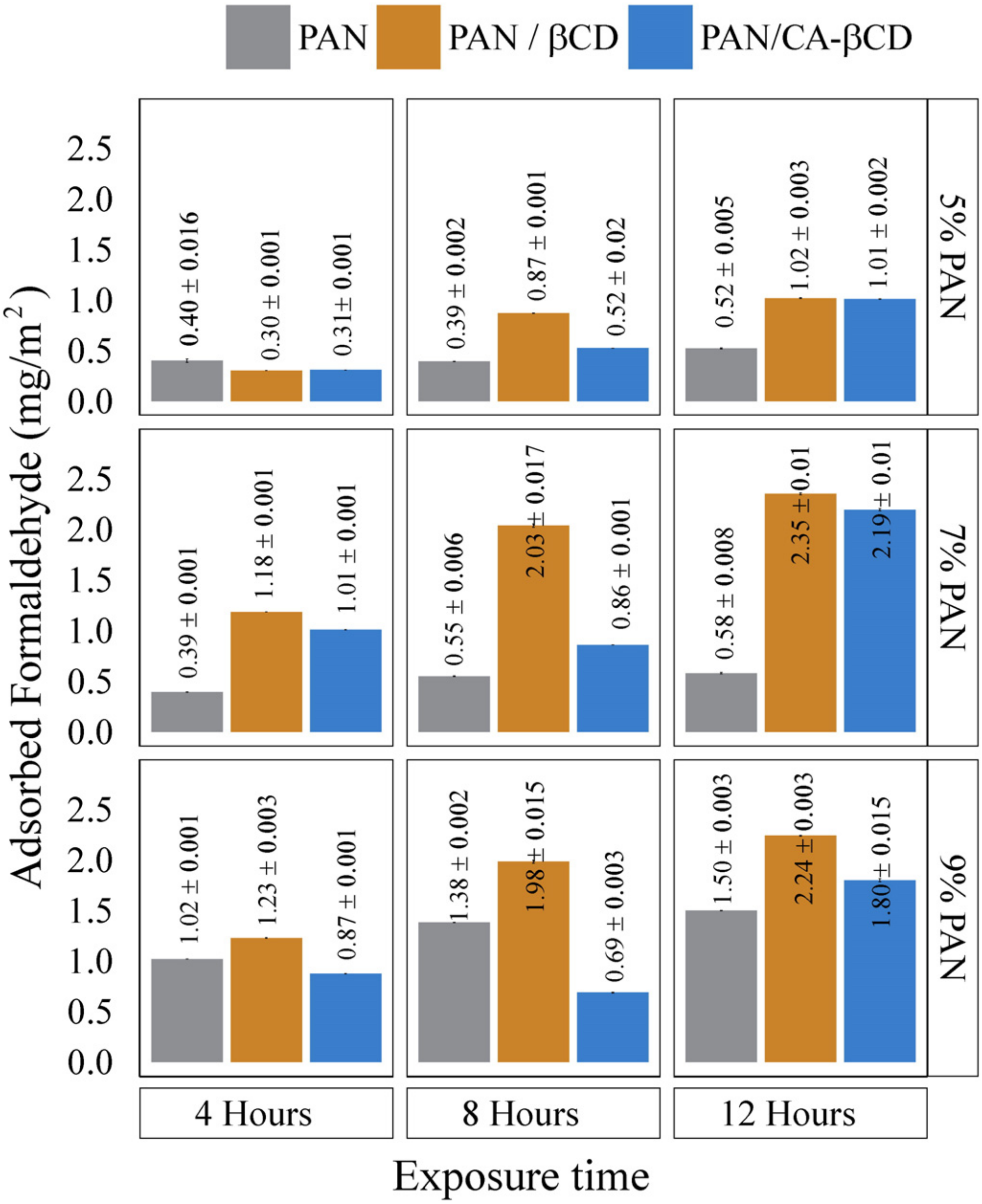

Fig. 8. Formaldehyde capture by PAN, PAN/βCD and PAN/CA-βCD nanofibers.

Unmodified and functionalized electrospun PAN nanofibers are mainly mesoporous structures with some micropores that could entrap small molecules. The surface area and the pore volume of PAN nanofibers are reduced when they are functionalized but the formaldehyde capture potential of electrospun PAN nanofibers is improved when they are physically functionalized with CD during the preparation of the polymer solution. The improvement in the formaldehyde capture potential of these fibers may be due to the free hydroxyl groups from the cyclodextrin molecule included in the polymer fiber. The formaldehyde capture capacity of PAN nanofibers is not improved when the βCD is crosslinked to the polymer by the chemical functionalization process presented in this paper. This may have happened because the free hydroxyl groups on the βCD molecule were modified during the esterification process. Considering the thermal resistance of the nanofibers, the addition of βCD to the polymer solution before the electrospinning process is also the best alternative for the functionalization of electrospun PAN nanofibers with βCD.

Based on the results presented in this work, we can conclude that physically functionalized PAN/βCD electrospun nanofibers may have potential as molecular filters for the capture of formaldehyde from the atmosphere. Besides, the amount of this contaminant than can be adsorbed by PAN/βCD nanofibers after 12 h of exposition in the testing atmosphere is almost the same when fibers are obtained from PAN/DMSO solutions with 7% *w*/w and 9% *w*/w PAN concentration. This means that βCD functionalized PAN nanofibers with average fiber diameters from 432 nm to 647 nm may have potential as indoor air purification materials. Finally, our results suggest that the capturing of formaldehyde by CD occurs on the external hydrophilic part of the molecule and not in the inner hydrophobic part.

Acknowledgment

Authors would like to thank to EAFIT University (621 - 000082) for the financial support of this research.

References

[1] W.D.P. Rengga, H. Sudibandriyo, M. Nasikin, Adsorption of low-concentration formaldehyde from air by silver and copper nano-particles attached on bamboo-based activated carbon, Int. J. Chem. Eng. Appl. (2013) 332–336, http://dx.doi.org/10.7763/IJCEA.2013.V4.320.

[2] Y. Song, W. Qiao, S.-H. Yoon, I. Mochida, Q. Guo, L. Liu, Removal of formaldehyde at low concentration using various activated carbon fibers, J. Appl. Polym. Sci. 106 (4) (2007) 2151–2157, http://dx.doi.org/10.1002/app.26368.

[3] K.J. Lee, N. Shiratori, G.H. Lee, J. Miyawaki, I. Mochida, S.-H. Yoon, J. Jang, Activated carbon nanofiber produced from electrospun polyacrylonitrile nanofiber as a highly efficient formaldehyde adsorbent, Carbon 48 (15) (2010) 4248–4255, http://dx.doi.org/10.1016/j.carbon.2010.07.034.

[4] OSHA, Osha fact sheet: formaldehyde URL https://www.osha.gov/OshDoc/data_General_Facts/formaldehyde-factsheet.pdf

[5] J. Pei, J.S. Zhang, On the performance and mechanisms of formaldehyde removal by chemi-sorbents, Chem. Eng. J. 167 (1) (2011) 59–66, http://dx.doi.org/10.1016/j.cej.2010.11.106.

[6] V. Boonamnuayvitaya, S. Sae-ung, W. Tanthapanichakoon, Preparation of activated carbons from coffee residue for the adsorption of formaldehyde, Sep. Purif. Technol. 42 (2) (2005) 159–168, http://dx.doi.org/10.1016/j.seppur.2004.07.007.

[7] L. Zehua, Y. An, M. Ranran, Removal of indoor pollutants by nano TiO2/beta-cyclodextrin coated paper under UV irradiation: Bioinformatics and Biomedical Engineering (iCBBE), 2010 4th International Conference on, IEEE, pp. 1–4. (URL http://ieeexplore.ieee.org/xpls/abs_all.jsp?arnumber=5516657)

[8] Z.-M. Huang, Y.-Z. Zhang, M. Kotaki, S. Ramakrishna, A review on polymer nanofibers by electrospinning and their applications in nanocomposites, Compos. Sci. Technol. 63 (15) (2003) 2223–2253, http://dx.doi.org/10.1016/S0266-3538(03)00178-7.

[9] A. Greiner, J. Wendorff, Electrospinning: a fascinating method for the preparation of ultrathin fibers, Angew. Chem. Int. Ed. 46 (30) (2007) 5670–5703, http://dx.doi.org/10.1002/anie.200604646.

[10] T. Uyar, R. Havelund, Y. Nur, J. Hacaloglu, F. Besenbacher, P. Kingshott, Molecular filters based on cyclodextrin functionalized electrospun fibers, J. Membr. Sci. 332 (1) (2009) 129–137, http://dx.doi.org/10.1016/j.memsci.2009.01.047.

[11] J. Szejtli, Introduction and general overview of cyclodextrin chemistry, Chem. Rev. 98 (5) (1998) 1743–1754.

[12] T. Uyar, R. Havelund, Y. Nur, A. Balan, J. Hacaloglu, L. Toppare, F. Besenbacher, P. Kingshott, Cyclodextrin functionalized poly(methyl methacrylate) (PMMA) electrospun nanofibers for organic vapors waste treatment, J. Membr. Sci. 365 (1) (2010) 409–417, http://dx.doi.org/10.1016/j.memsci.2010.09.037.

[13] T. Uyar, F. Besenbacher, Electrospinning of cyclodextrin functionalized polyethylene oxide (PEO) nanofibers, Eur. Polym. J. 45 (4) (2009) 1032–1037, http://dx.doi.org/10.1016/j.eurpolymj.2008.12.024.

[14] A. Celebioglu, S. Demirci, T. Uyar, Cyclodextrin-grafted electrospun cellulose acetate nanofibers via “click” reaction for removal of phenanthrene, Appl. Surf. Sci. 305 (2014) 581–588, http://dx.doi.org/10.1016/j.apsusc.2014.03.138.

[15] F. Kayaci, T. Uyar, Electrospun polyester/cyclodextrin nanofibers for entrapment of volatile organic compounds, Polym. Eng. Sci. 54 (12) (2014) 2970–2978, http://dx.doi.org/10.1002/pen.23858.

[16] F. Kayaci, T. Uyar, Electrospun zein nanofibers incorporating cyclodextrins, Carbohydr. Polym. 90 (1) (2012) 558–568, http://dx.doi.org/10.1016/j.carbpol.2012.05.078.

[17] S. Wang, J. Bai, C. Li, J. Zhang, Functionalization of electrospun ß-cyclodextrin/polyacrylonitrile (PAN) with silver nanoparticles: broad-spectrum antibacterial property, Appl. Surf. Sci. 261 (2012) 499–503, http://dx.doi.org/10.1016/j.apsusc.2012.08.044.

[18] T. Uyar, R. Havelund, Y. Nur, J. Hacaloglu, F. Besenbacher, P. Kingshott, Molecular filters based on cyclodextrin functionalized electrospun fibers, J. Membr. Sci. 332 (1) (2009) 129–137, http://dx.doi.org/10.1016/j.memsci.2009.01.047.

[19] F. Kayaci, Z. Aytac, T. Uyar, Surface modification of electrospun polyester nanofibers with cyclodextrin polymer for the removal of phenanthrene from aqueous solution, J. Hazard. Mater. 261 (2013) 286–294, http://dx.doi.org/10.1016/j.jhazmat.2013.07.041.

[20] D. Norena-Caro, M. Alvarez-Lainez, Experimental design as a tool for the manufacturing of filtering media based on electrospun polyacrylonitrile/b-cyclodextrin fibers, Int. J. Interact. Des. Manuf. (2015) http://dx.doi.org/10.1007/s12008-014-0241-4.

[21] V.A. Dyatlov, T.A. Grebeneva, I.R. Rustamov, A.A. Koledenkov, N.V. Kolotilova, V.V. Kireev, B.M. Prudskov, Hydrolysis of polyacrylonitrile in aqueous solution of sodium carbonate, Polym Sci. Ser. B 54 (3) (2012) 161–166, http://dx.doi.org/10.1134/S1560090412030050.

[22] W. Bao, Z. Xu, H. Yang, Electrokinetic and permeation characterization of hydrolyzed polyacrylonitrile (PAN) hollow fiber ultrafiltration membrane, Sci. Chin. Ser. B Chem. 52 (5) (2009) 683–689, http://dx.doi.org/10.1007/s11426-009-0064-5.

[23] H. Zhang, H. Nie, D. Yu, C. Wu, Y. Zhang, C.J.B. White, L. Zhu, Surface modification of electrospun polyacrylonitrile nanofiber towards developing an affinity membrane for bromelain adsorption, Desalination 256 (1) (2010) 141–147, http://dx.doi.org/10.1016/j.desal.2010.01.026.

[24] Y. Zhang, Q. Wu, H. Zhang, J. Zhao, Intelligent hydrophilic nanoparticles fabricated via alkaline hydrolysis of crosslinked polyacrylonitrile nanoparticles, J. Nanoparticle Res. 15 (7) (2013) http://dx.doi.org/10.1007/s11051-013-1800-5.

[25] K. Eltahlawy, M. Gaffar, S. Elrafie, Novel method for preparation of ß-cyclodextrin/grafted chitosan and it's application, Carbohydr. Polym. 63 (3) (2006) 385–392, http://dx.doi.org/10.1016/j.carbpol.2005.08.057.

[26] C. Dong, Y. Ye, L. Qian, G. Zhao, B. He, H. Xiao, Antibacterial modification of cellulose fibers by grafting ß-cyclodextrin and inclusion with ciprofloxacin, Cellulose 21 (3) (2014) 1921–1932, http://dx.doi.org/10.1007/s10570-014-0249-8.

[27] C. Dong, L.-Y. Qian, G.-L. Zhao, B.-H. He, H.-N. Xiao, Preparation of antimicrobial cellulose fibers by grafting ß-cyclodextrin and inclusion with antibiotics, Mater. Lett. 124 (2014) 181, http://dx.doi.org/10.1016/j.matlet.2014.03.091.

[28] USEPA, Method 8315a: determination of carbonyl compounds by high performance liquid chromatography (hplc) URL http://www.epa.gov/epawaste/hazard/testmethods/sw846/pdfs/8315a.pdf.

[29] S. Ramakrishna, An introduction to electrospinning and nanofibers, World Sci. (2005).

[30] O. Yordem, M. Papila, Y. Menceloglu, Effects of electrospinning parameters on polyacrylonitrile nanofiber diameter: an investigation by response surface methodology, 29 (1) (2008) 34–44, http://dx.doi.org/10.1016/j.matdes.2006.12.013 (URL http://linkinghub.elsevier.com/retrieve/pii/S0261306906003967).

[31] E. Gliscinska, B. Gutarowska, B. Brycki, I. Krucinska, Electrospun polyacrylonitrile nanofibers modified by quaternary ammonium salts, J. Appl. Polym. Sci. 128 (1) (2013) 767–775, http://dx.doi.org/10.1002/app.38210.

[32] Z. Kurban, A. Lovell, D. Jenkins, S. Bennington, I. Loader, A. Schober, N. Skipper, Turbostratic graphite nanofibres from electrospun solutions of PAN in dimethylsulphoxide, Eur. Polym. J. 46 (6) (2010) 1194–1202, http://dx.doi.org/10.1016/j.eurpolymj.2010.03.015.

[33] O. Yördem, M. Papila, Y. Menceloglu, Effects of electrospinning parameters on polyacrylonitrile nanofiber diameter: an investigation by response surface methodology, Mater. Des. 29 (1) (2008) 34–44, http://dx.doi.org/10.1016/j.matdes.2006.12.013.

[34] K. Nasouri, H. Bahrambeygi, A. Rabbi, A.M. Shoushtari, A. Kaflou, Modeling and optimization of electrospun PAN nanofiber diameter using response surface methodology and artificial neural networks, J. Appl. Polym. Sci. 126 (1) (2012) 127–135, http://dx.doi.org/10.1002/app.36726.

[35] D. Norena-Caro, M. Alvarez-Lainez, Solvent analysis in the fabrication of polyacrylonitrile/cyclodextrin (pan/cd) fibers by electrospinning, Remarks at the IUPAC World Polymer Congress — MACRO, 2014 (Chiang Mai, Thailand).

[36] Z.-M. Huang, Y.-Z. Zhang, M. Kotaki, S. Ramakrishna, A review on polymer nanofibers by electrospinning and their applications in nanocomposites, Compos. Sci. Technol. 63 (15) (2003) 2223–2253, http://dx.doi.org/10.1016/S0266-3538(03)00178-7.

[37] S. Nataraj, K. Yang, T. Aminabhavi, Polyacrylonitrile-based nanofibers—a state-of-the-art review, Prog. Polym. Sci. 37 (3) (2012) 487–513, http://dx.doi.org/10.1016/j.progpolymsci.2011.07.001.

[38] S. Dong, P. Dasgupta, Solubility of gaseous formaldehyde in liquid water and generation of trace standard gaseous formaldehyde, Environ. Sci. Technol. 20 (6) (1986) 637–640, http://dx.doi.org/10.1021/es00148a016.